



Survivability assessment of spacecraft impacted by orbit debris

Di-qi Hu ^{a, *}, Bao-jun Pang ^{a, *}, Run-qiang Chi ^a, Zhang-chi Song ^{a, b}, Hao Wu ^{a, c}

^a Hypervelocity Impact Research Center, Harbin Institute of Technology, 150080, Harbin, China

^b Beijing Institute of Aerospace Automatic Control, 100854, Beijing, China

^c Changchun Institute of Optics, Fine Mechanics and Physics, Chinese Academy of Sciences, 130033, Changchun, China

ARTICLE INFO

Article history:

Received 12 January 2020

Received in revised form

21 April 2020

Accepted 1 June 2020

Available online xxx

Keywords:

Survivability

Hypervelocity impact

Orbit debris

Ray method

ABSTRACTS

To help optimize the spacecraft design and reduce the risk of spacecraft mission failure, a new approach to assess the survivability of spacecraft in orbit is presented here, including the following three steps: 1) Sensitivity Analysis of spacecraft. A new sensitivity analysis method, a ray method based on virtual outer wall, is presented here. Using rays to simulate the debris cloud can effectively address the component shadowing issues. 2) Component Vulnerability analysis of spacecraft. A function “Component functional reduction degree – Component physical damage degree” is provided here to clearly describe the component functional reduction. 3) System-level Survivability Assessment of spacecraft. A new method based on expert knowledge reasoning, instead of traditional artificial failure tree method, is presented here to greatly improve the efficiency and accuracy of calculation.

© 2020 China Ordnance Society. Production and hosting by Elsevier B.V. on behalf of KeAi Communications Co. This is an open access article under the CC BY-NC-ND license (<http://creativecommons.org/licenses/by-nc-nd/4.0/>).

1. Introduction

Due to the increased space activities, orbit debris poses growing threats to space environment. The number of objects in Earth orbit officially cataloged by the U.S. Space Surveillance Network by the end of May, 2019 is nearly 20000 [1], yet only less than one fourth among those are active spacecrafts. However, those cataloged are simply the tip of the iceberg because the total amount of orbit debris, including those untraceable ones whose size are less than 10 cm, reaches more than 40 million [2] (see Fig. 1).

The orbit debris out of detection are of large quantity, and may cause major damages to spacecrafts. The highest speed of orbit debris when colliding with a spacecraft may reach as high as 16 km/s, and their average speed in Low earth Orbit is around 10 km/s. Once collision happens, the damages, from an inflection or a hole in components of a spacecraft to the functional degradation of the spacecraft, or even to its complete malfunction and catastrophic breakup, are all possible. Since each component of a spacecraft is closely related with its system and subsystems, any malfunction or functional degradation of a component may cause the equal

damage as that of a system. As we can see from Fig. 2, a solar wing of international space station was hit by orbit debris [3], causing the damage of one single bypass diode. Due to the malfunction of the bypass diode, the solar cells around it got overheated and was charred to an area about 36 cm long, contributing to the separation between Kapton material and substrate, which eventually resulted in the malfunction of the whole 400 solar cells.

Therefore, each Spacecraft designers, when designing a spacecraft, will evaluate the risks faced by spacecraft during its orbiting. Taking MM/OD (Micro Meteoroid and Orbital Debris) as the collision risk culprit, this paper will examine its collision probabilities to the internal components or systems of a spacecraft, in other words, to test the collision sensibility of a spacecraft. And PNP [4] (Probability of No Penetration) is taken as the failure criterion to examine the failure probabilities of the components or systems of a spacecraft. If an internal component or a system in a spacecraft is penetrated by MM/OD, it will be deemed as a failure according to PNP. Since it is not very difficult to conduct in practice, the method has been widely accepted and used in the world.

The United States was the first country to start such researches. In 1990s, the Americans, with reference to the previous study results of survivability in aircraft, developed the first spacecraft risk assessment software under MM/OD—BUMPER [5], which was widely and successfully employed in the risk assessment of many spacecrafts including space stations, space shuttles, Long Duration Exposure and Hubble Space Telescope. Through years of

* Corresponding author. Hypervelocity Impact Research Center, Harbin Institute of Technology, 92 Xidazhi Road, Harbin City, 150080, Heilongjiang, China.

E-mail address: pangbj@hit.edu.cn (B.-j. Pang).

Peer review under responsibility of China Ordnance Society

<https://doi.org/10.1016/j.dt.2020.06.003>

2214-9147/© 2020 China Ordnance Society. Production and hosting by Elsevier B.V. on behalf of KeAi Communications Co. This is an open access article under the CC BY-NC-ND license (<http://creativecommons.org/licenses/by-nc-nd/4.0/>).

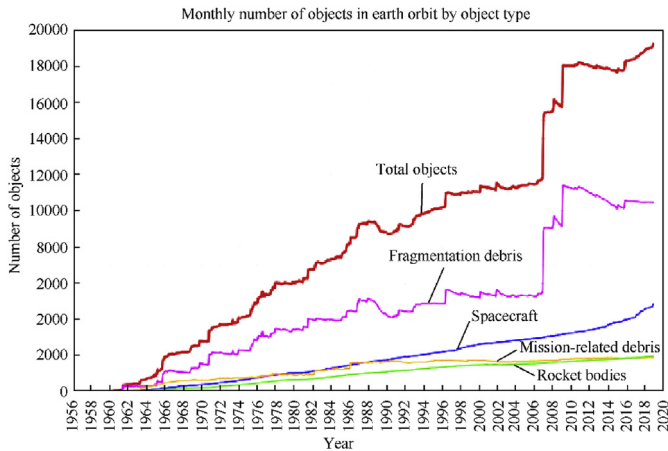


Fig. 1. A summary of all objects in Earth orbit officially cataloged by the U.S. Space Surveillance Network.

accumulating research, the software has been upgraded to BUMPER III [6], with more elaborate MM/OD Environmental engineering model, better impact tests and simulations on the vulnerability assessment of spacecraft both in components and in structures. Furthermore, BUMPER III can calculate the diameter and depth of impact crater, as well as the aperture if perforation happens. And equations of any crater or aperture size can be specified in the form of a subroutine.

ESABASE, a risk assessment software, was developed by ESA in 1992 and updated to ESABASE2 [7] in 1998. In ESABASE2, Monte Carlo method was used to analyze MM/OD flux. Due to the fact that some parts of a spacecraft are shadowing other parts, while previous software can hardly evaluate these components being shadowed, the greatest feature of ESABASE software is using a debris cloud module and a secondary ejecta module to address this issue. It employs a ray-tracking method — using the ray to represent the trail of debris, which can assess the effect of ejecta produced by primary impact from space debris, as well as the effect of secondary debris cloud. In addition, the size calculation of impact crater and impact perforation are also included in ESABASE2.

It is worth mentioning that both BUMPER III and ESABASE2 have upgraded and enriched their own space environment models. Taking the MM/OD threat of lunar orbit into consideration [8], both made the risk assessment on lunar orbit and on spacecrafts on the surface of moon under the NASA SP-8013 lunar ejecta environment. Furthermore, the impact of other factors such as 3rd Body Perturbation was also taken into consideration during the assessment.

MODAOST [9] developed by Chinese Academy of Space Science and Technology, was put into operation in 2005. This is the first software in China to analyze the impact probability and failure probability of orbit debris impacting on spacecrafts. MODAOST,

based on the PATRAN pre-processing software, developed the function of finite element modeling. The software also includes the iteration program of protective design and the optimizer of protective structure, which can optimize the design of spacecraft structures and improve their on-orbit survivability.

In 2008, Beijing Institute of Technology developed the orbit debris collision risk assessment system MODRAS [10]. The software, which integrates ORDEM2000 orbit debris environment model software, TrueGrid finite element modeling and other related service software, has a good user interface. Based on Roberts algorithm and Z buffer algorithm of computer graphics, a geometric processing method to shadowing problems is established, and the risk assessment of spacecraft on-orbit operation under MM/OD environment can also be carried out.

The above four risk assessment software are all based on Ballistic Limit Equations [11] (BLE) as damage criteria to determine whether the component fails or not under the high-speed impact of MM/OD. But this evaluation method does not take the functional reduction of components after impact into consideration, and components after impact does not necessarily lose efficacy. Therefore, the traditional PNP risk assessment method may not accurately evaluate the failure probability of both the components and the systems of spacecraft.

Vulnerability assessment software has been studied both at home and abroad. The vulnerability analysis software of HIV/AIDS [12] [(Hypervelocity Impact Vulnerability Area Model) and PIRAT [13] (Particle Impact Risk and Vulnerability Assessment Tool) have been developed in the United States and Germany respectively. The Vulnerability Analysis Software TVAS [14] (Target Vulnerability Analysis Software) and S³DE [15] (Survivability of Spacecraft in Orbit debris Environment) have also been developed by China Aerodynamic Research and Development Center and the Orbit debris High Speed Impact Research Center of Harbin University of Technology. To have better engineering application, these vulnerability analysis softwares simplify the failure modes accordingly, leading to the deficiencies in terms of the diversity of failure modes.

To help establish a better assessment method, a new spacecraft survivability assessment method is proposed in this article. The key point is how to assess the component vulnerability of spacecraft. Here we divide the components of spacecraft into structural components and functional components. Structural components are the components that provide configuration for the spacecraft body, bear and transmit loads, and still maintain certain stiffness and dimensional stability. They are the main frameworks of spacecraft. Functional components refer to the instruments or equipment that can achieve certain functions in space missions. In vulnerability analysis, structural components are characterized by BLE using PNP failure criterion. The vulnerability of functional components is characterized by establishing a quantitative relationship between the physical damage degree and efficiency attenuation degree. Finally, according to the characteristics of the functional structures

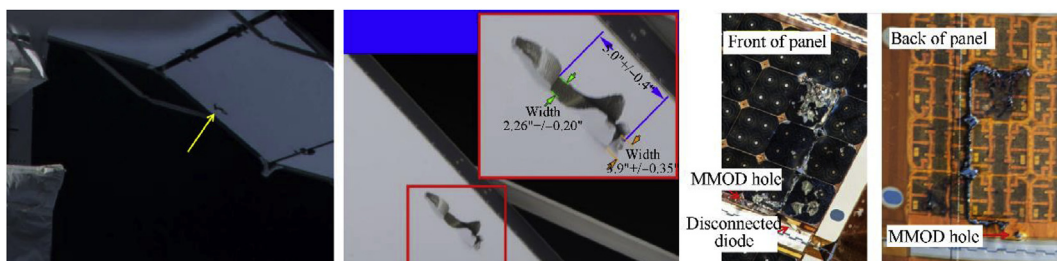


Fig. 2. A solar wing of international space station hit by orbit debris.

of the spacecraft system, and the transitive relationship between functional components, the probability of functional degradation or failure for the whole spacecraft under MM/OD (whether in low earth orbit or in geostationary orbit) can be obtained, that is, spacecraft survivability.

2. Overall scheme for spacecraft survivability assessment

Spacecraft survivability assessment involves the following three steps: sensitivity analysis under MM/OD environment, vulnerability analysis, and system-level survivability assessment of spacecraft.

The overall scheme of spacecraft survivability assessment is shown in Fig. 3. The Sensitivity Analysis refers to: using the orbit debris environmental engineering model, under specified orbital parameters, the MM/OD data is generated and then allocated to each initial ray; whether the initial ray intersects spacecraft or not is the criterion to judge whether MM/OD hits spacecraft. If the ray intersects with the spacecraft component, the next step is to check whether the component is penetrated and whether debris clouds are generated. If the debris penetrates the spacecraft at a relatively low velocity without any breaking, all we need to do is to calculate the residual velocity and mass, then using a new ray to represent it to continue the calculation. But if the debris penetrates the spacecraft at a high velocity and breaks, it will produce debris clouds, as shown in Fig. 4. And then the secondary debris cloud module will be used to create new rays to represent those debris clouds to continue the calculation. (the details of how “secondary debris cloud” works will be elaborated on in later chapters.)

The vulnerability analysis firstly establishes the quantitative relationship between the physical damage degree and the efficiency attenuation degree of each spacecraft component. When the ray intersects with the functional components of spacecraft, it will be calculated whether the components can be penetrated, and then through the quantitative relationship, the failure mode and failure probability of the components will be determined.

Spacecraft system-level survivability assessment method is based on expert-knowledge reasoning. Firstly, the failure knowledge base and the relational database of the whole failure tree are established. Then, with the failure knowledge base under the rules of the database, the failure modes and failure probability of the components obtaining from the previous step vulnerability analysis will be matched and inferred by inference machine. Finally, the failure mode and failure probability of the whole system is obtained.

3. Environmental engineering model of orbit debris

The environmental engineering model of orbit debris [16] describes the law of orbit debris flux, varying with debris size,

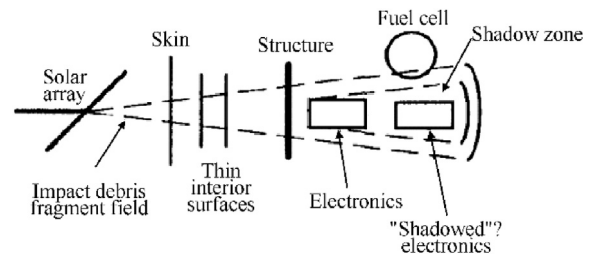


Fig. 4. Schematic diagram of secondary debris cloud generated by debris impact.

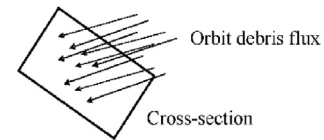


Fig. 5. Flux of orbit debris.

location, time and velocity by mathematical method, which provides necessary input conditions for subsequent calculation module. The flux F can be written as:

$$F(\Delta \vec{r}, \Delta \delta, \Delta \vec{v}) = \partial^2(q(t, \Delta \vec{r}, \Delta \delta, \Delta \vec{v})) / (\partial S \partial t) \quad (1)$$

F : the flux; q : the amount of debris; t : the time; $\Delta \vec{r}$: the spatial position, generally expressed by orbital elements; $\Delta \delta$: the size range of orbit debris; $\Delta \vec{v}$: the vector velocity of orbit debris, including the velocity range and direction; S : the cross-section area (see Figs. 5 and 6).

Existing orbit debris engineering models include: ORDEM 2000 of NASA series from America, MASTER model from ESA, SDPA-E model from Russia, and SDEEM2015 [17] from Harbin Institute of Technology in China. In this paper, SDEEM2015 and ORDEM2000 are used as the input model of orbit debris as impact risk source.

4. Sensitivity analysis of spacecraft based on ray method

4.1. Impact sensitivity analysis of spacecraft

The impact sensitivity of spacecraft components refers to the possibility of spacecraft components impacted by orbit debris. The impact sensitivity of any component is characterized by P_h , the probability of being hit by orbit debris or secondary debris.

Since the flux F under a certain range (the amount of orbit debris under specified range passing through a unit area per unit time) has been obtained, given the duration t , the expected value λ of the orbit debris passing through the cross-sectional area S can be

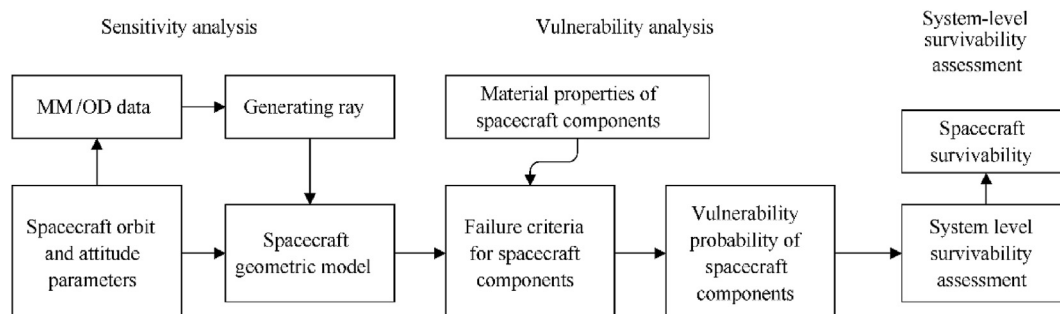


Fig. 3. Overall scheme for spacecraft survivability assessment.

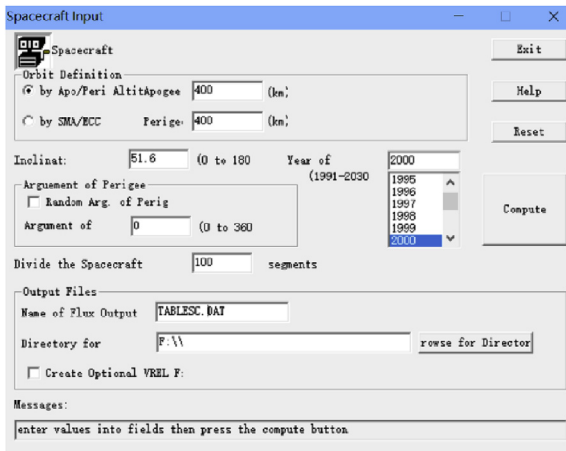


Fig. 6. ORDEM2000 software work interface.

expressed as

$$\lambda = FSt \quad (2)$$

It is assumed that the impact of orbit debris on a spacecraft meets the Poisson distribution [18]. Define n as the impact times, and the probability $P(n = k)$ can be written as:

$$P(n = k) = \frac{N^k e^{-N}}{k!}, k = 0, 1, 2, \dots \quad (3)$$

Among them, N is the mathematical expectation of impact; P is the corresponding probability. Therefore, the probability that no impact occurs $P(n = 0)$ is:

$$P(n = 0) = e^{-N} \quad (4)$$

And the probability that impact occurs at least once $P(n > 0)$ is:

$$P(n > 0) = 1 - e^{-n} \quad (5)$$

4.2. Virtual outer wall method and the generation of initial ray

4.2.1. Virtual outer wall method

The virtual outer wall method is to create a spherical region which includes the whole spacecraft in and then to divide the surface of the spherical region into several panels. The rays from these panels pointing to the spacecraft are generated with the angle of 10° between rays, which represent the direction of the incoming orbit debris (as shown in Fig. 7a). According to the data generated by the environment model of orbit debris, the impact flux of orbit

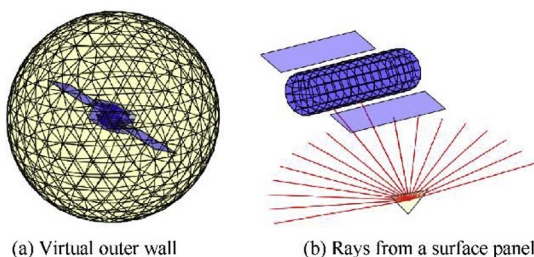


Fig. 7. Schematic diagram of virtual outer wall.

debris is distributed to these rays.

4.2.2. Ray pickup algorithm

Among the rays generated by the virtual outer wall panel (Fig. 7b), many rays fail to intersect with spacecraft while some of them have more than one points of intersection with spacecraft. During the process of sensitivity calculation, it is necessary to select the rays intersecting with the spacecraft, and to find out the first intersection point where the ray intersects the spacecraft with more than one intersection point. In this paper, Ray-Triangle cross-detection method [19] is used to pick up effective rays.

Defining the starting point of a ray as O and the unit direction vector as D , the ray $R(a)$ can be written as:

$$R(a) = O + aD \quad (6)$$

Defining the three points of a triangle as V_0, V_1, V_2 , the parametric equation $T(u, v)$ of the triangle can be expressed as:

$$T(u, v) = (1 - u - v)V_0 + uV_1 + vV_2 \quad (7)$$

$1 - u - v$: the weights of V_0 ; u : the weight of V_1 ; v : the weight of V_2 . And $u \geq 0, v \geq 0, u + v \leq 1$.

Therefore, the intersection point between ray $R(a)$ and the triangle must satisfy the equation:

$$O + aD = (1 - u - v)V_0 + uV_1 + vV_2 \quad (8)$$

Which is

$$\begin{bmatrix} -DV_1 - V_0V_2 - V_0 \\ a \\ v \end{bmatrix} = O - V_0 \quad (9)$$

Then the intersection point between the ray and the spacecraft can be calculated. For a ray with more than two intersection points, by comparing their location and depth, the intersection point with the smallest depth is where impact occurs.

4.3. Simulation verification of standard working conditions

Three standard working conditions are specified in the Protection Manual of orbit debris: cube satellites, spherical satellites and simplified space stations [6]. The size of the cube satellite is $1 \text{ m} \times 1 \text{ m} \times 1 \text{ m}$. The cross-sectional area of the spherical satellite is 1 m^2 . The simplified space station consists of one cube (the size is $1 \text{ m} \times 1 \text{ m} \times 1 \text{ m}$) and three cylinders (the diameter of the three cylinders is 1 m ; the length of the cylinder on the $-X$ axis is 3 m , and the length of the cylinder on the $-Y$ axis and the $+Z$ axis is 1 m). As shown in Fig. 7, it is a schematic diagram of the three standard working conditions.

To examine the validity of virtual outer wall method and the effectiveness of impact sensitivity analysis method based on virtual outer wall method, the sensitivity calculation of these three working conditions is carried out by using the algorithm provided in this paper, and the results are compared with that from the foreign vulnerability analysis software. Table 1 is the orbital parameters of spacecraft.

Table 2 shows the results of impact sensitivity under three standard working conditions. The total amount of debris larger than 0.1 mm and larger than 1 cm are recorded. The simulation results are compared with those from BUMPER and MDPANTO. From the results, it can be seen that the virtual external wall method and sensitivity evaluation method proposed in this paper are correct, and the results are in good agreement with the referenced analysis software. The maximum error is 2.67% , and the minimum error is 0.12% .

Table 1
Orbital parameters of spacecraft.

Orbit debris environment model	Orbit altitude/km	Orbit inclination/ $^{\circ}$	Eccentricity ratio	Launch year	On-track working years
ORDEM2000	400	51.6	0	2002	1

Table 2
Total number of collisions and impact sensitivity under three standard working conditions.

Working condition	debris size	algorithm in this paper	P_h	BUMPER	$\Delta\%$	MDPANTO	$\Delta\%$
Cube satellite	$d \geq 0.1$ mm	2.099E+01	1.000E+00	2.131E+01	1.50	2.139E+01	1.87
	$d \geq 1$ cm	2.841E-06	2.841E-06	2.876E-06	1.21	2.872E-06	1.07
Spherical satellite	$d \geq 0.1$ mm	1.669E+01	1.000E+00	1.695E-01	1.53	1.699E+01	1.76
	$d \geq 1$ cm	2.137E-06	2.137E-06	2.134E-06	0.14	2.141E-06	0.19
Simplified space station	$d \geq 0.1$ mm	9.098E+01	1.000E+00	9.176E+01	0.85	9.165E+01	0.73
	$d \geq 1$ cm	1.144E-05	1.44E-05	1.151E-05	0.61	1.149E-05	0.44

Figs. 8–10 show the impact sensitivity of spacecraft under three standard working conditions, and the pseudo-chromatogram of the collision number is used to show the impact sensitivity of the spacecraft. The velocity direction of the satellite is parallel to the y-axis. It can be seen from the figure that the impact sensitivity of the spacecraft is affected by the shadowing relationship among components. In the direction of debris inflow, the collision number on shielded spacecraft components is significantly less than that on unshielded components, which shows that the sensitivity algorithm can simulate the shadowing relationship (see Fig. 11).

5. Vulnerability analysis of spacecraft

The vulnerability analysis of spacecraft includes two parts: component-level and system-level analysis. And the components are further divided into structural and functional components. The component-level vulnerability analysis is to obtain the probability of components impacted by orbit debris under different failure modes. Each mode corresponds to a damage criterion, which is a quantitative criterion to measure whether the function of components has been reduced or failed. The system-level vulnerability analysis is to obtain the probability of spacecraft failure of various levels under impact.

5.1. Vulnerability assessment of structural components

Structural components refer to the components that provide configuration for the spacecraft body, bear and transmit loads, and maintain a certain stiffness and dimensional stability, which are the main framework of the spacecraft. Structural components can provide support and interfaces for other subsystems to integrate with the main structure into a complete system [20]. Only physical damage will occur to this kind of structural components when impacted by orbit debris, neither damaging its function nor affecting other components. Therefore, the vulnerability of such

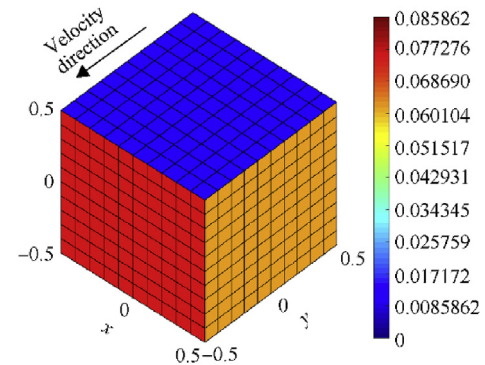


Fig. 9. Distribution of collision number of cube satellite ($d \geq 0.1$ mm).

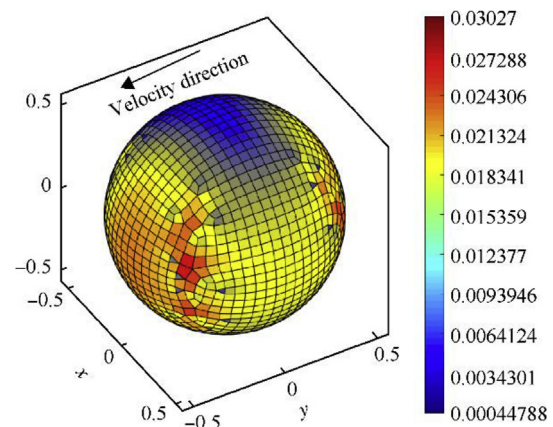


Fig. 10. Distribution of collision number of spherical satellite ($d \geq 0.1$ mm).

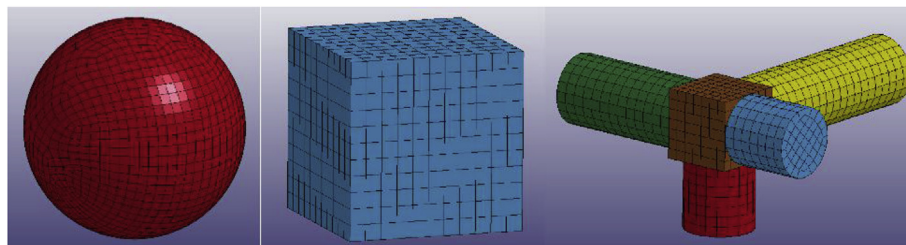


Fig. 8. Schematic diagram of three standard working conditions.

components can be calculated under the impact limit equation.

(1) Impact limit equation of single-layer plate

The current most widely used impact limit equation of single-layer plate is the improved Cour-Palais equation [21]:

$$d_c = \left[\frac{t_s \cdot BH^{0.25} (\rho_s / \rho_p)^{0.5}}{k \cdot 5.24 (V \cos \theta / C)^{2/3}} \right]^{18/19} \quad (10)$$

where d_c is the critical fragment diameter; BH is Brinell Hardness; t_s is the thickness of target plate; ρ_s and ρ_p are respectively the density of the target plate and the projectile; C is the sound velocity of target plate; V is the fragment velocity; θ is the impact inclination angle and k is 1.8.

(2) Impact limit equation of Whipple protective structures [22].

Whipple protective structure is a typical protection scheme of orbit debris, which includes two layers of metal plates. The first layer is a buffer structure. After debris impact, secondary debris clouds are generated, and secondary debris clouds expand along

$$d_c = \begin{cases} \left[\frac{t_w / K_{3S} (\sigma_y / 40)^{1/2} + t_b}{0.6 (\cos \theta)^\delta \rho_p^{1/2} V^{2/3}} \right]^{18/19} & V \leq V_L \cos \theta \\ \frac{1.155 S^{1/3} t_w^{2/3} (\sigma_y / 70)^{1/3}}{K_{3D}^{2/3} \rho_p^{1/3} \rho_b^{1/9} V^{2/3} (\cos \theta)^\delta} & V \geq V_H \cos \theta \\ d_c(V_L) + \frac{[d_c(V_H) - d_c(V_L)]}{V_H - V_L} \cdot (V - V_L) & V_L \leq V / \cos \theta \end{cases} \quad (12)$$

Among them, the corresponding parameters of the honeycomb structure of different materials are different, as shown in Table 3:

5.2. Vulnerability assessment of spacecraft functional components

The current widely used failure criterion for components is to examine the equivalent thickness of aluminum alloy plates under the same impact. If the equivalent target plates are penetrated, the component failure occurs. And the impact limit can be obtained by the impact limit equation of single layer plate.

Probability of component failure under given impact is:

$$P_{k/h} = \begin{cases} 1, \text{equivalent thickness of aluminum alloy plate}^3 \text{ impact limit} \\ 0, \text{equivalent thickness of aluminum alloy plate} < \text{impact limit} \end{cases}$$

the velocity direction and impact on the bulkhead. As the action area increases, the energy is dispersed and the damage to bulkhead is effectively reduced. Christiansen equation is the most widely used impact limit equation for double-deck plates:

This is a simplified model which is easy to be realized in engineering. But for the functional components of spacecraft, due to the

$$d_c = \begin{cases} 3.919 t_w^{2/3} s^{1/3} \rho_p^{-1/3} \rho_b^{-1/9} \left(\frac{\sigma}{70} \right)^{1/3} (V \cos \theta)^{-2/3} & \text{while } V_n < 3 \\ 1.07 t_w^{2/3} s^{1/3} \rho_p^{-1/3} \rho_b^{-1/9} \left(\frac{\sigma}{70} \right)^{1/3} \left(\frac{V \cos \theta}{4} - 0.75 \right) + \left\{ \frac{t_w \left(\frac{\sigma}{40} \right)^{0.5} + t_b}{1.248 \rho_p^{0.5} \cos \theta} \right\}^{18/19} \left(1.75 - \frac{V \cos \theta}{4} \right) & \text{while } 3 < V_n < 7 \\ \left\{ \left[t_w \left(\frac{\sigma}{40} \right)^{0.5} + t_b \right] / \left(1.248 \rho_p^{0.5} \cos \theta \right) \right\}^{18/19} & \text{while } V_n > 7 \end{cases} \quad (11)$$

where subscript b and w represent the parameters of the first layer and the second layer respectively; t is the thickness of the plate; ρ is the density, and σ is the yield strength of the back wall.

(3) Impact limit equation of Honeycomb sandwich panel [23].

Honeycomb sandwich panel is a widely used protective structure on satellite. It can be seen as a combination of Whipple structure and aluminum honeycomb core. Under high-speed impact, the front panel of honeycomb sandwich panel is broken and moves radially. Honeycomb core absorbs energy through plastic deformation, rupture and disintegration, which hinders the radial movement of debris cloud.

complexity of structures and the diversity of functions, when evaluating the damage degree of these functional components, it is difficult to characterize the functional reduction if the physical damage information is used to stand for the functional damage just like that in structural components. Therefore, how to study the functional reduction degree under the corresponding conditions based on the physical damage information has become the key to the vulnerability assessment of spacecraft functional components.

In order to illustrate the reduction degree of functional components more clearly and accurately, this paper provides a new approach. Firstly, taking the spacecraft environment into consideration, we need to select and calculate the effectiveness index in order to obtain the physical damage degree of the components, and then according to a certain mapping relationship [24], convert it

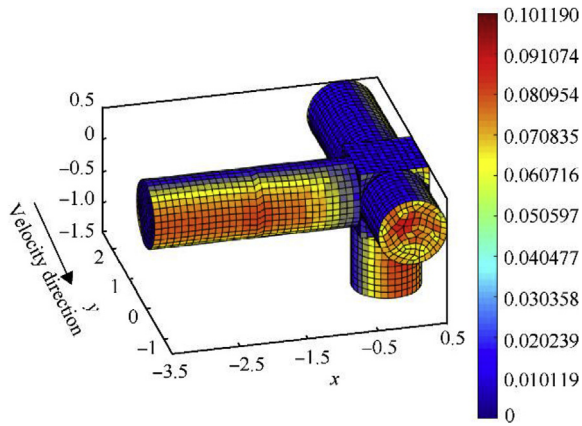


Fig. 11. Distribution of collision number of simplified space station ($d \geq 0.1$ mm).

into the efficiency value under the corresponding conditions, that is, the reduction degree of functional components. The efficiency reduction of the functional components is a mapping of its physical damage degree, which can be expressed by a function based on the physical damage information of the component. For typical components, the mapping relationship between their efficiency reduction and the physical damage degree of the target is very clear. Defining the physical damage degree of the component $P(x)$, the initial performance value of the component $u_0(x)$, and the efficiency value corresponding to its physical damage $u(x)$, then the relation between the efficiency reduction degree and the physical damage degree of the component can be written as:

$$\frac{u_0(x) - u(x)}{u_0(x)} = f\{P(x)\} \quad (13)$$

This index method can be used to obtain the mapping relation, yet the more specific expression of the mapping relation must be analyzed by taking the specific function of functional components and its operation environment into consideration. Therefore, this paper introduces the concept of efficiency attenuation degree to measure the reduction degree of the component efficiency, or to characterize the degree to which the component fails to function well; and the efficiency reduction degree is a fuzzy quantity, which can be expressed by membership degree. Obviously, the algorithm of efficiency reduction varied from different functional components. The membership function can generally be taken as an index function, that is:

$$\frac{u_0(x) - u(x)}{u_0(x)} = \alpha \exp\{\beta P(x)\} \quad (14)$$

where $u(x)$ is the efficiency reduction function; $0 \leq u(x) \leq u_0(x) \leq 1$; $P(x)$ is the physical damage information of the component; α and β are constants, and their values not only depend on the needs of the system, but also are related to the selection of damage effect index.

Taking the spacecraft battery as an example, when the battery is impacted to a complete failure, an aluminum plate can be used here

to show the equivalent effects which is clearer and more straightforward. And under this condition, the minimum thickness of equivalent aluminum plate is defined as P_0 . When the battery is impacted under real MM/OD conditions, P_1 is the thickness of an aluminum plate to show the equivalent effects.

Then we can get a ratio P :

$$P = \frac{P_1}{P_0} \quad (15)$$

If P is less than 1%, the battery is not affected; if P is 10%, the battery power is reduced by 30%; if P is 30%, the battery power is reduced by 50%; if P is more than 65%, the battery is completely disabled. Based on the above data, the efficiency reduction function through the above formula 14 can be determined as:

$$u(P) = \begin{cases} 1.0, & P < 0.01; \\ 1.0 - 0.01 \cdot 30^{-1/9} \exp\left[\frac{100}{9} \ln 30 P\right], & 0.01 \leq P \leq 0.1; \\ 1.0 - 0.3 \cdot \sqrt{\frac{3}{5}} \exp\left[5 \ln \frac{5}{3} P\right], & 0.1 < P \leq 0.3; \\ 1.0 - \frac{5}{18} \exp\left[\frac{10}{3} \ln \frac{5}{9} P\right], & 0.3 < P \leq 0.65; \\ 0, & P > 0.65. \end{cases} \quad (16)$$

5.3. Simulation of debris cloud by ray method

The debris cloud model describes the debris details in the debris cloud formed by the hypervelocity impact of orbit debris on the satellite structure, which can provide a basis for the simulation of the hypervelocity impact behavior of debris. The debris cloud model proposed by the China Center for Aerodynamic Research and Development describes debris clouds in terms of velocity, mass and spatial angle distribution of debris. The model includes the functions of debris cloud front velocity, debris mass distribution, debris rate distribution, debris space angle distribution and so on [25].

As shown in Fig. 12, the initial debris moves at a speed V along the positive direction of the x -axis, and the position of target plate crosses the origin and is perpendicular to the xOy plane, the angle of whose normal with the x -axis is θ . α is the angle between the debris velocity vector and the positive direction of the y -axis, and β is the angle between the projection of the debris velocity vector on the xOz plane and the negative direction of the z -axis.

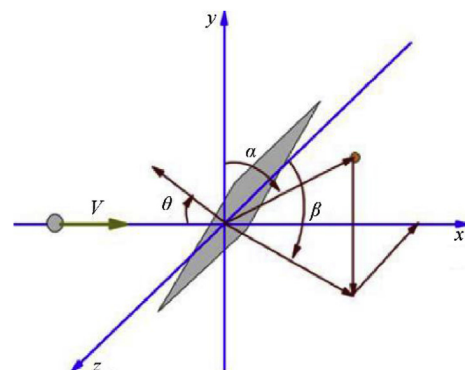


Fig. 12. Schematic diagram of description parameters of spatial location of debris in debris cloud.

Table 3
Parameters of impact limit equation for honeycomb structures.

materials	V_L	V_H	K_{3D}	K_{3S}	δ
Aluminum/other	3	7	1.4	0.4	$4/3$ ($45^\circ \leq \theta \leq 65^\circ$)
CFRP	4.2	8.4	1.1	0.4	$5/4$ ($45^\circ \leq \theta \leq 65^\circ$) $4/3$

The maximum impact velocity of debris produced by a debris cloud can be expressed as

$$V_{\max}(t/D, V, \theta) = \left(\sum_{i=0}^2 ad_i \times (t/D)^i \right) \times \left(\sum_{i=0}^2 av_i \times V^i \right) \times \left(\sum_{i=0}^2 as_i \times \cos(\theta)^i \right) - k_0 \frac{(t/D)^{k_1}}{\cos(\theta)^{k_2}} \quad (17)$$

$CN(m)$ is defined as the ratio of the debris number with mass less than or equal to m to the total number of debris cloud fragments, that is,

$$CN(m) = 1 - \left(\sum_{i=0}^2 ad_i \times (t/D)^i \right) \times \left(\sum_{i=0}^2 av_i \times V^i \right) \times \left(\sum_{i=0}^2 as_i \times \cos(\theta)^i \right) \times \left[\left(\sum_{i=0}^2 ad_i \times (t/D)^i \right) \times \left(\sum_{i=0}^2 av_i \times V^i \right) \times \left(\sum_{i=0}^2 as_i \times \cos(\theta)^i \right) \right]^{m-3} \quad (18)$$

$CN(v)$ is defined as the ratio of the debris number with velocity less than or equal to v to the total number of debris cloud fragments, that is,

$$CN(v) = v^{0.895} \quad (19)$$

$CN(\alpha)$ and $CN(\beta)$ is defined as the ratio of the debris number whose angle equals respectively to α and β to the total number of debris cloud fragments, that is,

$$n(\alpha) = \frac{A_\alpha \times \exp\left(-2\left(\frac{\alpha-90-k \times \theta}{w_{la}}\right)^2\right)}{w_{la} \sqrt{\frac{\pi}{2}}} + \frac{(1-A_\alpha) \times \exp\left(-2\left(\frac{\alpha-90-k \times \theta}{w_{la}}\right)^2\right)}{w_{la} \sqrt{\frac{\pi}{2}}} \quad (20)$$

$$n(\beta) = \frac{\exp\left(-2\left(\frac{\beta-90}{w_\beta}\right)^2\right)}{w_\beta \sqrt{\frac{\pi}{2}}} \quad (21)$$

There are upper and lower bounds for α and β in the debris cloud, and the formula are:

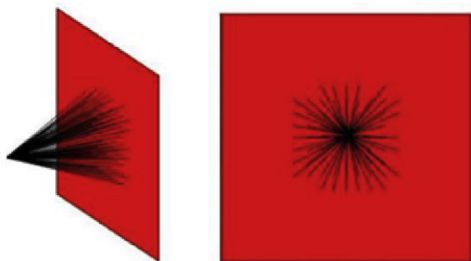


Fig. 13. Schematic diagram of sub-rays of fragment cloud.

$$\begin{cases} \alpha_{\max}(\theta, v) = g(\theta, v) + f(\theta, v) \\ \alpha_{\min}(\theta, v) = g(\theta, v) - f(\theta, v) \\ \beta_{\max}(\theta, v) = g(\theta, v) + f(\theta, v) \\ \beta_{\min}(\theta, v) = g(\theta, v) - f(\theta, v) \\ g(\theta, v) = 90 + \theta - \frac{\theta}{2}v \\ f(\theta, v) = \frac{90 + p_1 v^{0.5}}{1 + p_2 v + p_3 v^{0.5}} + (1 - \cos \theta) \left[90 - kv - \frac{90 + p_1 v^{0.5}}{1 + p_2 v + p_3 v^{0.5}} \right] \end{cases} \quad (22)$$

According to the distribution function of debris cloud, the random simulation samples of debris parameters are obtained by inverse transform sampling [26]. First of all, the initial debris impact position is taken as the starting point of the sub-ray, and the space angles α and β are taken as 5° , 10° , 15° , 175° , with 1156 spatial directions in total. Then, according to the upper and lower bound function in the debris cloud model, the rays that exceed the upper and lower bounds are eliminated, and the effective sub-rays are obtained, as shown in Fig. 13.

The expected value of the momentum of a single fragment in a debris cloud is calculated according to formulas 18 and 19:

$$E(mv) = \iint mnCN'(m)CN'(v)dmdv \quad (23)$$

According to the conservation of momentum, the expected number of fragments is calculated:

$$E(N) = mv / E(mv) = mv / \iint mnCN'(m)CN'(v)dmdv \quad (24)$$

After many times of inverse transform sampling on $CN(m)$, $CN(v)$, $f n(\alpha)$ and $f n(\beta)$, the fragment parameters of the composite distribution are obtained. Each set of fragment parameters is assigned to the rays with the closest spatial angle parameter.

6. System-level survivability assessment of spacecraft

Based on the above analysis and calculation, we obtain the damage probability of each component. The most widely used system-level survivability assessment method is failure tree analysis, which uses the downlink method or uplink method to find out the system failure that leads to the top failure event. The corresponding logical relationship is used to connect them. Finally, a tree logic diagram is formed, as shown in Fig. 14, which shows the failure tree of the power system.

The advantage of this method is clear and simple, but every time a spacecraft is evaluated, the logical relationship of failure tree must be re-established, which is complicated. Therefore, an improved method based on expert knowledge reasoning is presented here, as shown in Fig. 15. The failure event database of spacecraft system and the failure tree database of spacecraft systems and subsystems are established. The probability of component failure degree and functional reduction degree calculated by spacecraft vulnerability analysis is taken as the input data. Matching the data with the two databases, an effective failure tree model is automatically generated. With the calculation and analysis, the extent and probability of spacecraft failure and functional reduction is finally generated.

The establishment of the knowledge base subsystem [27] is the core part of the evaluation method. The main task is to standardize the expert knowledge of the survivability of the spacecraft system. The expert knowledge is inputted into the computer according to certain rules, and the system has editing functions such as viewing,

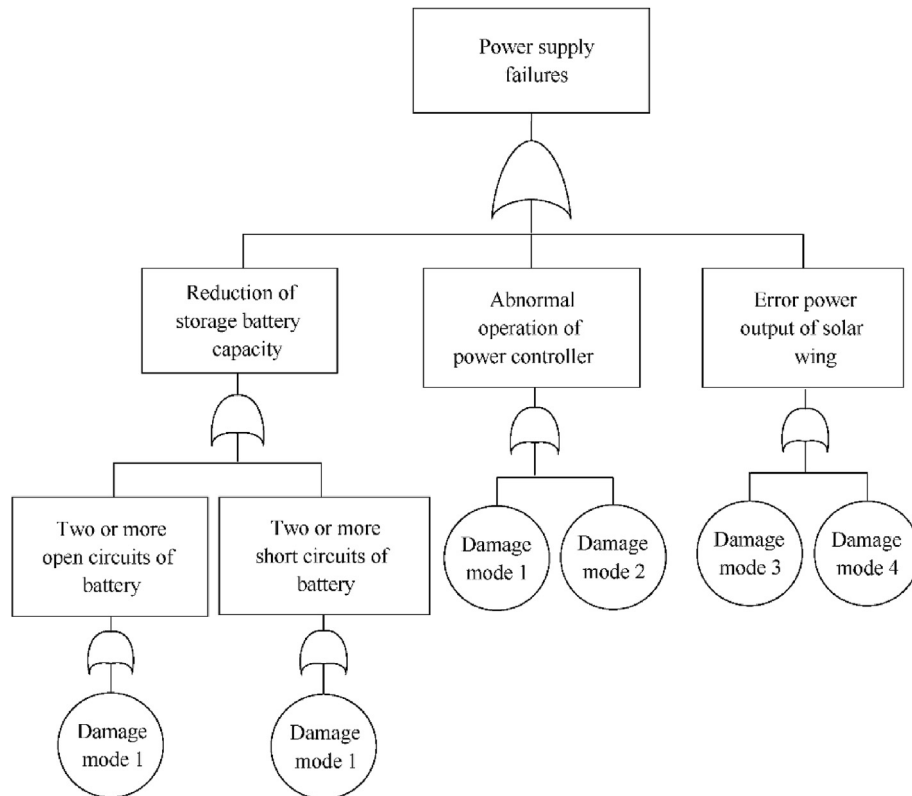


Fig. 14. Power system failure tree.

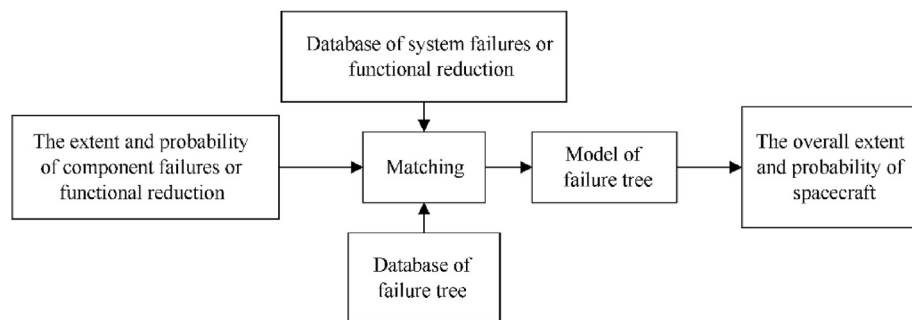


Fig. 15. Flow chart of survivability assessment based on expert knowledge reasoning.

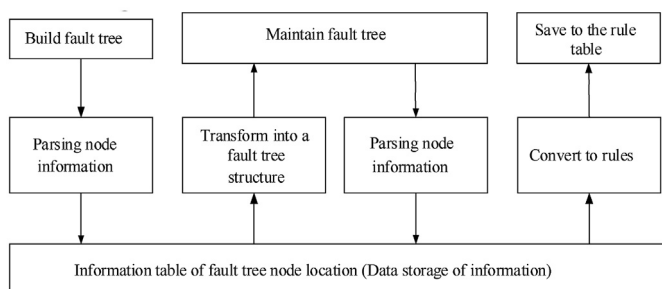


Fig. 16. Flow chart of knowledge base establishment based on fault tree.

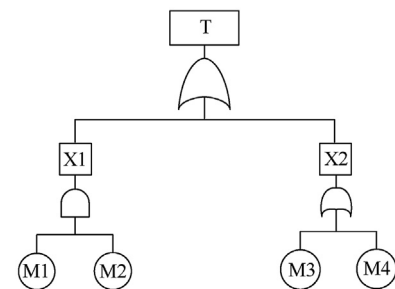


Fig. 17. Diagram of fault tree structure.

adding, deleting and modifying. The process is shown in Fig. 16.

The certain rules [28] in the expert system of the fault tree is the rules to represent the fault tree in computer in the form of minimum cut set. The diagram of fault tree structure can be expressed in Fig. 17 as follows:

Rule 1:IF M1 AND M2 THAN X1
 Rule 2:IF M3 THAN X2
 Rule 3:IF M4 THAN X2
 Rule 4:IF X1 THAN T
 Rule 5:IF X2 THAN T

In the calculation process of system-level survivability, in order to obtain the uncertain relationship of system damage caused by component damage, the credibility condition should be added when describing the rules, so it is necessary to rewrite the above rules in the following form:

IF P THEN Q (CF(Q,P))

Among them, CF (Q, P) is the probability of the occurrence of Q when P occurred, which can be expressed not only by accurate numerical values, but also by the experience of experts.

7. Conclusions

A ray method to assess the survivability of spacecraft under the impact of orbit debris is proposed in this paper. The sensitivity analysis of spacecraft based on virtual outer wall method is proposed, and the ray method to simulate the secondary debris cloud model is established to solve the shadowing problem between spacecraft components. The function between the efficiency reduction degree and physical damage degree of the components are established to characterize the functional reduction of the functional components, which solves the perplexing problem that the vulnerability of the spacecraft can only be characterized by 0–1. Finally, the system survivability assessment based on expert knowledge reasoning is used instead of the original artificial failure tree method, which greatly improves the efficiency. The spacecraft survivability evaluation method in this paper reveals new sights for spacecraft designers to optimize the design and reduce the mission risk.

Declaration of competing interest

The authors declare that they have no known competing financial interests or personal relationships that could have appeared to influence the work reported in this paper.

References

[1] NASA Orbital Debris Program Office. Orbital Debris Quart News 2019;23(1):

- 12–3. <https://orbitaldebris.jsc.nasa.gov/quarterly-news/pdfs/odqnv23i1.pdf>.
- [2] Du Heng, Zhang Wenxiang, Pang Baojun, et al. Orbit debris. Beijing: China Aerospace Press; 2007. p. 1–20.
- [3] Christiansen E. MMOD protection and degradation effects for thermal control systems. 2014. <https://ntrs.nasa.gov/archive/nasa/casi.ntrs.nasa.gov/20140010668.pdf>.
- [4] Christiansen Eric L, et al. Handbook for designing MMOD protection, NASA TM-2009-214785. Houston TX: NASA Johnson Space Center; 2009, June.
- [5] Wang Haifu, Feng Shunshan, Liu Youying. Introduction to orbit debris. Beijing: The Science Publishing Company; 2010. p. 198.
- [6] Christiansen Eric L, Nagy, et al. Bumper 3 update for IADC protection manual. 2016. <https://ntrs.nasa.gov/archive/nasa/casi.ntrs.nasa.gov/20160003137.pdf>.
- [7] Ruhl K, Bunte KD, Gaede A, et al. ESABASE2-Debris software user manual. 2014. p. 10–21. <https://esabase2.net/wp-content/uploads/2015/12/ESABASE2-Debris-User-Manual.pdf>.
- [8] Gäde A, Miller A. ESABASE2/Debris release 7.0 technical description. 2015. p. 9–15. <https://esabase2.net/wp-content/uploads/2015/12/ESABASE2-Debris-Technical-Description.pdf>.
- [9] Han Zengyao, Zheng Shigui, Yan jun, et al. Development, calibration and application of orbit debris impact probability analysis software. J Astronaut 2005;(2):228–231+243.
- [10] Wang Haifu, Yu Qingbo, Liu Youying. Orbital debris risk assessment system. Trans Beijing Inst Technol 2008;28(12):1039–42.
- [11] IADC WG3. Protection manual. IADC-04-03, version 7.0. September 19,2014.
- [12] P.E. Nebolsine, E.Y. Lo, D. Svenson. Satellite component vulnerability model, AIAA 96-4239.
- [13] Scott Kempf, Frank Schäfer, Rudolph Martin, et al. Risk and vulnerability analysis of satellites due to MM/SD with PIRAT. In: 6th European conference on orbit debris, Darmstadt, Germany; 2013.
- [14] Zhou Zhi-xuan, Huang Jie, Ren Lei-sheng. A vulnerability analysis method of spacecraft under orbit debris impact. In: 67th international astronautical congress, vol. 9. Mexico: Guadalajara; 2016.
- [15] Ma Zhenkai. Spacecraft survivability to orbit debris risk. Harbin Institute of Technology; 2017.
- [16] Liou JC, Matney MJ, Anz-Meador PD, et al. The new NASA orbital debris engineering model ORDEM2000. 2002.
- [17] Wang Dongfang. Research on the forecast of space debris environment. Harbin Institute of Technology; 2014.
- [18] Welty N, Rudolph M, Schäfer F, et al. Computational methodology to predict satellite system-level effects from impacts of untrackable orbit debris. Acta Astronaut 2013;88:35–43.
- [19] Möller T, Trumbore B. Fast, minimum storage ray/triangle intersection. J Graph Tool 1997;2(1):21–8.
- [20] Ding Li. Study of ballistic limit of dual-wall shadowing structures against orbit debris. Harbin Institute of Technology; 2008.
- [21] Ryan S, Christiansen EL. A ballistic limit analysis programme for shadowing against micrometeoroids and orbital debris. Acta Astronaut 2011;69:245–57.
- [22] Christiansen EL. Design and performance equation for advanced meteoroid and debris shields. Int J Impact Eng 1993;14:145–56.
- [23] Schonberg William, FrankSchäfer, Putzar Robin. Hypervelocity impact response of honeycomb sandwich panels. Acta Astronaut 2010;66:455–66.
- [24] Li Qixin, Xiang Aihong, Li Hongxia. Calculation and assessment on damage effect of system target. Acta Armamentarii 2008;(1):57–62.
- [25] Huang J, Ma ZX, Ren LS, et al. A new engineering model of debris cloud produced by hypervelocity impact. Int J Impact Eng 2013;56(56):32–9.
- [26] Kuhl ME. History of random variate generation. In: 2017 winter simulation conference (WSC). IEEE; 2017. p. 231–8.
- [27] Du Jie. Research on expert system implementation of railway signal equipment fault diagnosis based on fault tree analysis. Beijing Jiaotong University; 2009.
- [28] Lu Zhi, Yang Jun. Implementation of aerospace equipment diagnosis system based on fault tree and rule. J Comput Appl 2015;35(S2):181–4.